# Reports

## Molecular Dynamics Simulation of a Phospholipid Micelle

J. J. WENDOLOSKI, S. J. KIMATIAN, C. E. SCHUTT, F. R. SALEMME

**The dynamic character of phospholipid aggregates limits conventional structural studies to the determination of average molecular features. In order to develop more detailed descriptions of phospholipid structure for comparison with experiment, the molecular dynamics of a hydrated lysophosphatidylethanolamine (LPE) micelle, incorporating 85 LPE and 1591 water molecules, have been simulated. Comparison of the initial and equilibrated micelles shows substantial differences both in LPE hydrocarbon chain conformation and polar head-group–solvent interactions. Although these changes produce only subtle effects on the averaged structural properties of the system, the alterations in hydrocarbon chain packing and head-group solvation appear to mimic a polymorphic pretransition from a spherical toward a cylindrical micelle structure.**

POLYMORPHIC CHANGES IN MEMbrane phospholipids are supposed to cause the transient formation of pores, vesicles, or lipoprotein complexes involved in many aspects of cell function (*1, 2*). The structural origins of these transitions are poorly understood at the molecular level. This lack of detail primarily reflects the dynamic character of phospholipid aggregates, which limit x-ray (*3*) or neutron (*4*) scattering experiments to the determination of average molecular features. Here we describe computer simulations that provide an alternative method for studying the detailed behavior of molecules in complex systems, and in the micelle case suggest how events occurring at the molecular level produce polymorphic transitions in phospholipid aggregates.

Micelles are assemblies of amphiphilic molecules whose polar head groups are exposed to solvent and whose aliphatic chains pack compactly in the hydrophobic micelle interior. An important conceptual issue is to evaluate how the balance between the forces stabilizing the surface and those stabilizing the hydrophobic core affects micelle organization. We have investigated this question by performing molecular dynamics simulations on a micelle model, constructed from LPE monomers known to form micelles in aqueous solution (*2*), that conforms to the commonly held notion of a radially symmetric structure. This model differs from previous simulations (*5–8*) in that the LPE monomers include zwitterionic head groups capable of forming a hydrogen-bonded surface network among themselves and with solvent molecules.

The LPE monomer conformation was derived from the crystal structure (*9*) of dilaurylphosphatidylethanolamine (DLPE) by replacement of the fatty acid substituent at the central glycerol oxygen with a hydroxyl group. The model was assembled by aligning the extended hydrocarbon chains of the LPE molecules along radii of a sphere whose diameter was equal to the DLPE crystal bilayer thickness (48 Å), and by including enough replicates (85 total) so that the surface area per phospholipid head group was similar to that of the DLPE crystal structure. By design, a number greater than 60 guarantees that the molecules are nonequivalent, thus avoiding bias toward icosahedrally symmetric contacts. The initial model was then energy minimized and hydrated with a two-layer shell of 1591 water molecules.

Although the initial structure had a high energy due to unfavorable steric clashes near the micelle center, unconstrained energy minimization rapidly produced a sterically acceptable structure (Fig. 1A). At this early, pre-equilibrated stage of the 125-ps simulation, the structure is stabilized by polar interactions formed between LPE zwitterionic head groups oriented tangent to the spherical micelle surface. Despite the restraining effects of the network of head-group interactions, both the glycerol linkers and fatty acid chains are flexible enough to

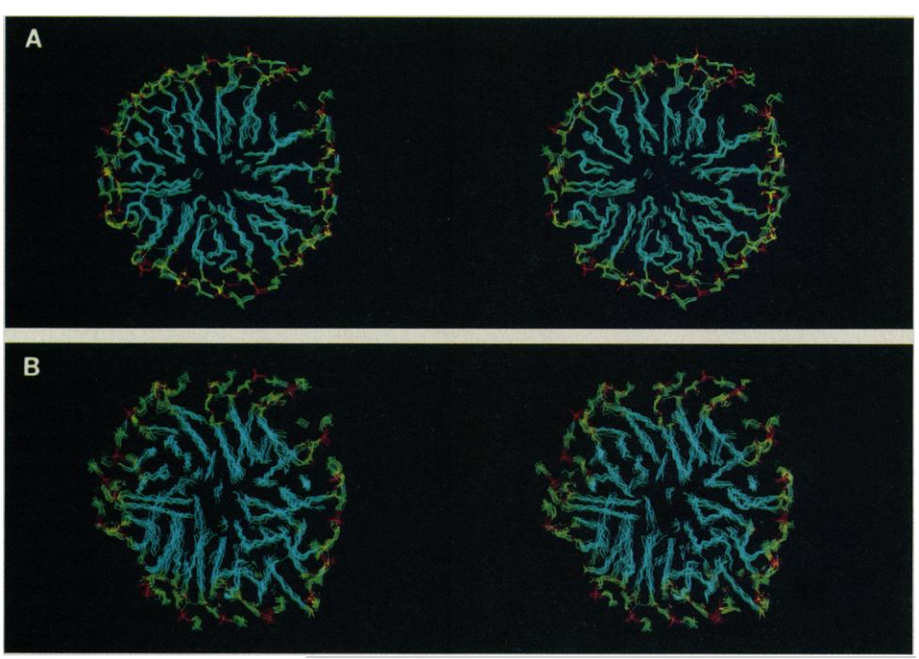


**Fig. 1.** Stereoviews of micelle molecular dynamics. The frames show 13 Å thick sections of the micelle as a superposition of ten frames spanning (**A**) 0 to 5 ps, and (**B**) 35 to 40 ps of the 125-ps simulation. Water molecules surrounding the micelle are omitted in the illustration. White bonds on the periphery of the micelle correspond to hydrogen bonds formed directly between the LPE zwitterionic head groups. Hydrogen bonds of this type are much more extensive in (A) than in (B). The initial structure was minimized by performing 5000 steps of energy minimization with the phosphorus atoms constrained to their initial positions, followed by 5000 steps of unconstrained minimization. The system was then solvated with a two-layer water shell (*19*) and again minimized for 5000 steps. The solvated system was heated to 300 K over a period of 3 ps, equilibrated for 22 ps, and dynamics simulated for an additional 100 ps. All calculations were performed using AMBER (*20, 21*) interfaced to the GEMM (*22*) system. The initial nonsolvated minimizations used a distance-dependent dielectric constant of 4 (*21*).

J. J. Wendoloski and F. R. Salemme, E. I. du Pont de Nemours & Company, Central Research and Development Department, Experimental Station, Wilmington, DE 19880.
S. J. Kimatian and C. E. Schutt, Department of Chemistry, Princeton University, Princeton, NJ 08544.

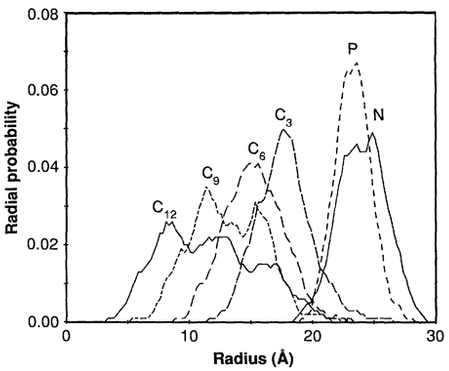


**Fig. 2.** Time-averaged radial probability functions for selected LPE atoms averaged at 0.05-ps intervals for the last 100 ps of the dynamics simulation. The curves represent the relative probability of finding a given atom at a specified distance from the center of the micelle. Distributions are shown for the N and P atoms of the zwitterionic LPE head group, and the fatty acid carbons $C_3$, $C_6$, $C_9$, and $C_{12}$ (carbon atoms are numbered from the carboxylic acid end of the fatty acid group).

permit compact packing of the micelle interior, allowing fatty acid chains to incorporate gauche conformations in order to fill voids near the micelle surface. Overall, the micelle in the early stages of equilibration resembles the interphase radial lattice model described by Dill and Flory (*10, 11*), in which the LPE dipole network fixes the origins of hydrocarbon chains on the spherical micelle surface and the hydrocarbon chains assume a distribution of extended and gauche conformations required to pack the micelle interior.

The pre-equilibrium LPE micelle is organized by a dipolar surface lattice similar to that which stabilizes the bilayer organization of DLPE crystals (*9*). However, the regularity of this network is disrupted during the initial few picoseconds of simulation because of water hydration of LPE head groups. The solvation process is reflected in a reduction of the number of hydrogen bonds formed between the LPE zwitterionic head groups. The initial micelle (Fig. 1A) is stabilized by some 340 hydrogen bonds, or an average of four bonds per head group. At later stages of the simulation, the total number of hydrogen bonds fluctuates around 250 ± 10. Concomitant with the disruption of the polar head-group interactions, the LPE hydrocarbon chains straighten and associate more compactly in extended clusters (Fig. 1B). The cluster chains pack locally on a hexagonal grid, although the packing is distorted on the larger scale by relative staggering and twisting between chains. The equilibrated micelle can thus be described as an aggregate of a small number of such clusters plus a few isolated chains lying in the hydrophobic grooves between them. Once formed, the clusters are relatively stable on the 100-ps time scale of the simulation.

The time evolution of the micelle is reflected in the number and distribution of gauche bonds in the LPE fatty acid chains. On average, the hydrocarbon chains in the equilibrated micelle have fewer gauche bonds per chain than those in the initial structure (Table 1), but the gauche bonds that do occur tend to be localized near the glycerol linkers (Table 2). This structure allows the head groups to swivel in order to achieve an orientation consistent with the fairly continuous hydrophilic barrier around the ordered straight chain clusters in the core (Fig. 1B), while maximizing hydrogen bonding and close packing.

Despite the relative regularity of the internal chain packing in the LPE micelle, the time-averaged radial probability functions (Fig. 2) show increasingly broad distributions for atoms nearer the end of the hydrophobic tail. This distribution, predicted by the interphase models of micelle structure (*12, 13*), has been observed in previous micelle dynamics simulations of surfactants with shorter hydrocarbon chains (*5–8*) and is consistent with experimental observations of micelles in solution (*14*). In general, such distributions have been taken as representing only trans-gauche conformational statistics of individual LPE hydrocarbon chains. However, in the present case, the distribution also reflects larger scale "rocking and rolling" of the LPE clusters relative to one another, "flattening" of the spheroid, and the effects of the intercluster molecules. The radial probability function thus appears to be a relatively insensitive indicator of detailed micelle chain organization, although it fits the experimental scattering data (*6*).

The clustering of the LPE molecules resembles "pie wedges" and is compatible with the observed tendency for lysophospholipids to aggregate into cylindrical micelles (*15*). In this sense the LPE simulation can be viewed as approximating a polymorphic pretransition from a spherical micelle, whose organization is dominated by surface dipole interactions, toward a "cylindrical" micelle, stabilized by a more uniform compact packing of the fatty acid chains. Indeed, similar transitions have also been observed in model monolayer simulations (*16*). Although computer-generated, this transition illustrates how environmental factors such as hydration can affect dynamic organization of phospholipid molecules and result in polymorphism. From this perspective, it becomes clear how variations in molecular structure that influence either trans-gauche conformational equilibria (for example, incorporation of unsaturated bonds that act like fixed gauche bonds in the fatty acid chains) or the extent to which head groups can interact potentially determine overall aggregate structure. The application of statistical mechanics to the problem of micelle stability (*17, 18*) has thus far been limited to relatively simple mean-field models because of the paucity of precise structural data. The kind of clustered packing of "quasi-equivalent" molecules revealed in the present simulation provides a good approximation for a more detailed theory of lipid polymorphism.

This micelle transition also provides a basis for understanding how proteins binding through ionic interactions to the phospholipid aggregate surface can either enhance or destabilize head-group interactions to bring about polymorphic transitions. Alternatively, proteins inserting stiff structures like α helices into the hydrophobic core could effect polymorphic transitions by nucleating and stabilizing ordered aggregation of the fatty acid chains. Future computational experiments are aimed at testing this hypothesis in detail.

**Table 1.** Probability of finding a given number of gauche bonds in one chain.

| Number of gauche bonds | Initial micelle* | Equilibrium micelle† |
|---|---|---|
| 0 | 0.12 | 0.38 |
| 1 | 0.18 | 0.38 |
| 2 | 0.22 | 0.13 |
| 3 | 0.11 | 0.08 |
| 4 | 0.18 | 0.03 |
| 5 | 0.13 | 0.00 |
| 6 | 0.04 | 0.00 |
| 7 | 0.02 | 0.00 |
| 8 | 0.00 | 0.00 |

*Average over the initial 5 ps of the dynamics simulation. †Average over final 100 ps of the dynamics simulation (sampled in 0.05-ps increments).

**Table 2.** Probability of finding a given bond in the gauche configuration.

| Bond | Initial micelle* | Equilibrium micelle† |
|---|---|---|
| C1–C2 | 0.40 | 0.36 |
| C2–C3 | 0.37 | 0.14 |
| C3–C4 | 0.27 | 0.09 |
| C4–C5 | 0.31 | 0.13 |
| C5–C6 | 0.34 | 0.10 |
| C6–C7 | 0.32 | 0.08 |
| C7–C8 | 0.25 | 0.05 |
| C8–C9 | 0.31 | 0.04 |
| C9–C10 | 0.15 | 0.03 |

*Average over initial 5 ps of the dynamics simulation. †Average over final 100 ps of the dynamics simulation (sampled in 0.05-ps increments).


REFERENCES AND NOTES

1. B. de Kruiff, *Nature* **329**, 587 (1987).
2. J. N. Israelachvili, S. Marcelja, R. G. Horn, *Q. Rev. Biophys.* **13**, 121 (1980).
3. V. Luzzati, T. Gulik-Krzywicki, A. Tardieu, *Nature* **218**, 1031 (1968).

4. S.-H. Chen, *Annu. Rev. Phys. Chem.* **37**, 351 (1986).
5. J. M. Haile and J. P. O'Connell, *J. Phys. Chem.* **88**, 6363 (1984).
6. M. C. Woods *et al.*, *ibid.* **90**, 1875 (1986).
7. B. Jonsson *et al.*, *J. Chem. Phys.* **85**, 2259 (1986).
8. K. Watanabe *et al.*, *J. Phys. Chem.* **92**, 819 (1988).
9. M. Elder, P. Hitchcock, R. Mason, C. G. Shipley, *Proc. R. Soc. London Ser. A* **354**, 157 (1977).
10. K. A. Dill and P. J. Flory, *Proc. Natl. Acad. Sci. U.S.A.* **77**, 3115 (1980).
11. ———, *ibid.* **78**, 676 (1981).
12. K. A. Dill *et al.*, *Nature* **309**, 42 (1984).
13. K. A. Dill and R. S. Cantor, *Macromolecules* **17**, 380 (1984).
14. T. Zemb and C. Chachaty, *Chem. Phys. Lett.* **88**, 68 (1982).
15. B. Owenson and L. R. Pratt, *J. Phys. Chem.* **84**, 2906 (1984).
16. J. P. Bareman, G. Cardini, M. L. Klein, *Phys. Rev. Lett.* **60**, 2152 (1988).
17. I. Szleifer *et al.*, *J. Chem. Phys.* **85**, 5345 (1986).
18. ———, *ibid.* **83**, 3612 (1985).
19. W. L. Jorgensen *et al.*, *ibid.* **79**, 926 (1983).
20. P. Weiner and P. A. Kollman, *J. Comput. Chem.* **2**, 287 (1981).
21. S. J. Weiner *et al.*, *J. Am. Chem. Soc.* **106**, 765 (1984).
22. B. R. Brooks, in *Supercomputer Research in Chemistry and Chemical Engineering*, C. Jensen and D. Truhlar, Eds. (American Chemical Society, Washington, DC, 1987), pp. 123–145.
23. We thank Z. Wasserman for analysis code development and R. Hilmer for computer graphics code (MOLEDITOR). C.E.S. thanks the American Heart Association and NIH for partial support.

17 August 1988; accepted 23 November 1988

# Critical Depth for the Survival of Coral Islands: Effects on the Hawaiian Archipelago

RICHARD W. GRIGG AND DAVID EPP

**Coral islands drown when sea level rise exceeds the maximum potential of coral reefs to grow upward (about 10 millimeters per year). During the Holocene transgression (18,000 years ago to present) sea levels rose at rates of up to 10 to 20 millimeters per year, and most coral island reefs situated deeper than a critical depth of 30 to 40 meters below present day sea level drowned. Coral islands that did not drown during the Holocene transgression apparently all developed on antecedent foundations shallower than critical depth. During low stands in sea level during the Pleistocene, these islands were elevated and subject to subaerial erosion. Today, in the Hawaiian Archipelago, the depth of drowned banks is inversely related to summit area; smaller banks are progressively deeper, evidently because of erosional truncation during low sea level stands. Bank summit area may therefore be an important factor determining the failure or success of coral islands.**

THE FORMATION OF CORAL ATOLLS has been generally understood since the work of Darwin (*1*). In Darwin's theory, a coral reef grows upward around a sinking volcano until the volcanic edifice subsides below sea level, leaving a coral atoll. However, among 261 atolls in the world's oceans, there are 116 drowned shallow banks, all suitable for the development of atolls (*2, 3*). Many of these banks have the shape of atolls and are at depths between 10 and 200 m. Why these banks drowned while others adjacent or nearby did not has been a long-standing question (*2, 4, 5*). In several atoll-guyot pairs, for example, Bikini and Sylvania, one edifice drowned and the other did not (*6, 7*). Schlager (*8*) has described the problem of reef drowning as a paradox because he suggested that the growth potential of reefs is capable of exceeding the rate of postglacial sea level rise. In this report, we redefine the problem, claiming that during cycles of glacio-eustacy, coral reefs that are situated on banks below a critical depth drown, but reefs growing on shallower foundations do not. We hypothesize that bank depth depends primarily on subaerial erosion which in turn depends on bank summit area and sea level history. We have tested this hypothesis against a set of data from drowned banks in the Hawaiian Archipelago.

The Hawaiian Archipelago is an ideal setting for the study of drowned coral reefs. The chain stretches west-northwest across the Pacific between 20°N and 29°N, from the island of Hawaii to Kure atoll, and contains eight high volcanic islands, five islets with broad banks, three atolls, two coral islands at sea level, and 25 drowned banks (Fig. 1). All of these edifices originated over a hotspot currently located near 19°N 155°W (*9, 10*). Although the archipelago is in tropical latitudes suitable for the development of coral reefs (*11*), some banks have drowned while others have not.

Processes contributing to changes in depth of coral reefs include reef growth, change in eustatic sea level, erosion, and subsidence or uplift of antecedent foundations (Tables 1 and 2). Coral reefs drown when sea level rise outpaces the rate of carbonate accumulation, minus subsidence and erosion, for periods long enough that reefs submerge below a "critical depth." Below this depth, coral reefs cannot maintain a positive net rate of upward accretion.

Sea level has undergone at least 17 cycles of transgression and regression during the Pleistocene (*12, 13*), all likely constrained within several tens of meters above and about 200 below present sea level (*14*). Most workers have estimated that the last sea level low stand in the Holocene was 120 to 135 m below present sea level (*13, 15–17*) (Fig. 2), but it may have been as much as 165 m lower (*18*). Between 18,000 and 9,000 years ago, the long-term average sea level rise was about 12 mm/year (*8, 14*); however, the rise may have been up to 20 mm/year during intervals spanning several thousand years (*18, 19*).

For comparison, maximum rates of net upward coral reef growth are generally about 10 mm/year or less (*13, 20–22*) (Table 1). Higher rates have been measured for maximum potential growth of corals in optimal environments (*23, 24*), but these are not representative of entire reefs. Highest rates of calcification for corals (and reefs) occur at depths of 5 to 10 m and decline rapidly with increasing depth (*25, 26*). At 30 m, rates of vertical growth of individual species of massive corals are between 15 and 40% of their rates at optimum depth (*24–26*). For example, in Jamaica, the rate of upward accretion of the entire reef at 30 m is 1.3 mm/year; about 20% of the rate at 10 m (*25, 27*). This low rate of carbonate production is close to average rates of biological and mechanical erosion (Table 2). Thus rates of sea level rise during the height of the Holocene transgression were greater than the maximum potential of coral reefs to grow upward, particularly if rates of erosion and subsidence are taken into account (Tables 1 and 2).

The critical depth for drowning for most coral reefs in the world is estimated to be about 30 to 40 m, but could be less depending on geographic differences in ecological factors such as light, temperature, sedimentation, turbidity, disturbance, and bioerosion (*8*). Darwin (*1*) recognized the significance of critical depth and called it the limit of vigorous growth. He placed it at a depth of 36 m. Vaughan and Wells (*28*) estimated the zone of vigorous growth to be less than 30 m. Buddemeier and Hopley (*29*) placed it at 40 m. Geologists, in many cases, have estimated that critical depth is deeper; between 50 and 100 m (*8, 30*). Deep-water coral species may survive at depths much greater than 40 m (*13, 31*) but entire reefs below this depth are generally unable to

R. W. Grigg, Hawaii Institute of Marine Biology, University of Hawaii, Honolulu, HI 96822.
D. Epp, National Science Foundation, 1800 G Street, NW, Washington, DC 20550.